Associated conference: 5th International Small Sample Test Techniques Conference

Conference location: Swansea University, Bay Campus

Conference date: 10th - 12 July 2018

How to cite: Moreno, D., Haroush, S., Turgeman, A. & Silverman, I. 2018. Small punch technique used to evaluate the radiation damage in SS316L thin foils due to proton bombardment. *Ubiquity Proceedings*, 1(S1): 36 DOI: https://doi.org/10.5334/uproc.36

Published on: 10 September 2018

Small punch technique used to evaluate the radiation damage in SS316L thin foils due to proton bombardment

D. Moreno [1], S. Haroush [2], A. Turgeman [2] and I. Silverman [1]

1 Soreq Nuclear Research Center, Yavne 70600, Israel

2 Nuclear Research Center-Negev, P.O. Box 9001, Beer-Sheva 84190, Israel
Affiliation 1; dmoreno@netvision.net.il
Affiliation 2; monih6655@gmail.com
***** Correspondence: dmoreno@netvision.net.il; Tel.: +972-50-629-2406

Abstract: The mechanical properties characterization of thin foils to be used as target in high intensity accelerator requires non standards techniques. Previous studies, focused on foils after annealed, cold rolled and heat treatment after rolled, in addition to foils at different thickness, have been carried out to estimate the sensitivity of the small punch test (SPT) technique in foils. In this research we studied the degradation of the mechanical properties of foils due to irradiation damage by high intensity proton beams. For this new study, two samples of SS316L foils have 25 μm thickness were exposed to proton bombardment at 3.6 MeV, and approximately 300 μA of current for a period of 3 hours and 40 hours, separately. The SPT technique revealed that the un-irradiated specimens exhibited the largest load and deformation before failure, rather than the irradiated foils. The electron microscopy observations (SEM) revealed high cross slips and pseudo-cleavage density combined with multiple deformation twinning after irradiation to high energy. The mechanical behavior can be explained by the microstructure. The crack propagation path is in a zigzag fracture mode when multiple deformation twinning occurs close to the stretched zone of the foil and failure. Changes of the SPT measurements were found and the degradation from ductile to brittle crack mode is attributed to radiation damage effects.

Keywords: radiation damage; SPT; mechanical properties, twin deformation, accelerator, proton, SARAF

---

1. Introduction

The Soreq Applied Research Accelerator Facility (SARAF) is a multi-user and versatile particle accelerator facility located at the Soreq Nuclear Research Center [1]. The beam operation on the thin-foil target is the subject of interest in the present work.

Thin foils (25μm) are used in cyclotron accelerators as a window for liquid and gas targets. Irradiation of targets by proton or deuteron beams is carried out at various energies and occasionally at high currents and for long time durations, up to a few hours. During such irradiation conditions, the foil might be damaged; its microstructure and mechanical properties can be degraded and, therefore, the window life-time can be significantly reduced.

The changes in the foils mechanical properties due to proton irradiation requires the characterization of its properties before and after the irradiation process in order to analyze the alloy's ability to withstand the process. The goals of the current stage of the research were to study the SS316L foil mechanical behavior in two different conditions of irradiation.

Small Punch Test (SPT), Ball Punch Test (BPT), Disk Bend Test (DBT) [4], and Shear Punch Test are common mechanical techniques for the characterization of small dimension or thin specimens [2–7]. These testing methods are usually conducted on specimens that are too small to undergo standard tension tests. The SPT concept is based on locking a thin sheet-like specimen between two dies and pushing a punch against it with a spherical cap, up until failure. During the test, the load and the punch stroke are monitored simultaneously until the end-test criterion (e.g., maximal or failure load) is achieved. Many of the common standards, including the E-643 ASTM standard, are valid for specimens whose thickness ranges from 200 to 2000 μm [8]. In many research publications focusing on mechanical characterization the specimen thickness is greater than 200 μm [9–13].

Haroush et al. [14] have shown that for specimens having a thickness greater than 300 μm, classical plate equations can be used to estimate the yield stress, while for thinner specimens yield stress estimation from SPT is a very complex issue, since it is a function of the specimen thickness.

To correlate between yield stress and ultimate stress obtained by SPT to tensile test, Finite Element Analysis (FEA) was applied using damage model as shown in [14]. To validate the FE model, the computed load displacement curves obtained from the FE computation were compared to the experimental curves. Interrupted SPT

experiments in which the experiment was terminated prior to specimen failure were conducted for the observation of deformed but un-cracked specimens that were cut and examined under a microscope.

In the present study we report the SPT results, the energy to fracture and the fracture modes by SEM observation of SS316L, 25 μm foils that were exposed to proton bombardment at 3.6 MeV, 300μA for 3 and 40 hours irradiation in the SARAF. The results show mechanical properties degradation and ductile to brittle fracture attributed to the radiation damage effects.

2. Materials and Methods

This study was carried out on foils of SS316L as targets. The foils following irradiation exhibited high activation as shown by auto radiography of the foil in figure 1b. Because the high activation we had to wait 5 years until the activation decreases and the foils return to the background level. Schematic apparatus for SPT is shown in figure 2a [15].

The SARAF accelerator was operated at 250 and 310 μA, 3.6 MeV CW beam of 4 W/mm^2 heat flux on a thin foil target of 25μm. Beam operation was focused on the thin foil target as shown in the calculation of the temperature in figure 1a. The main beam current limit was the foil surface maximum temperature that was limited to 500±50 ºC. This was achieved owing to the following two factors; development and improvement of the target design and improvement of the beam diagnostics system and the tuning procedures. Pattern on the foil at the higher current is due to the convection process in the cooling liquid NaK metal.

The temperature in the target region, the collected beam currents on the electrodes and neutron dose rates were monitored during operation. The temperatures were monitored using thermocouples probes and an optical pyrometer.

The small punch specimens were cut by scissors to W= L = 8 mm dimensions (figure 2a). The SPT was conducted using the apparatus shown in figure 2a by clamping of the specimen between the dies under 600 N, pre load up to 20 N and balance the stoke transducer (Instron COD), and finally pushing the ball into the specimen under stroke control at a speed of 0.2 mm/min up to failure [14-15]. The end test criterion was the drop from the maximal loads, this happening very sharply. The dimensions of the SPT apparatus are: the corner radius of the dies in the internal cylinders (close to de samples) R_D = 0.2 mm; the ball diameter $2r_b$ = 2.4 mm; the lower die internal cylinder diameter, $2R_{LD}$ = 3 mm and upper die cylinder diameter $2R_{UD}$ = 3.1 mm.

Following specimen failure, indicated by the load drop, the specimen shape, dimensions, and fracture mode were characterized by scanning electron microscopy (SEM). In addition, Cross section metallography using SEM reviled that considerable number of equiaxed grains presence across the thickness.

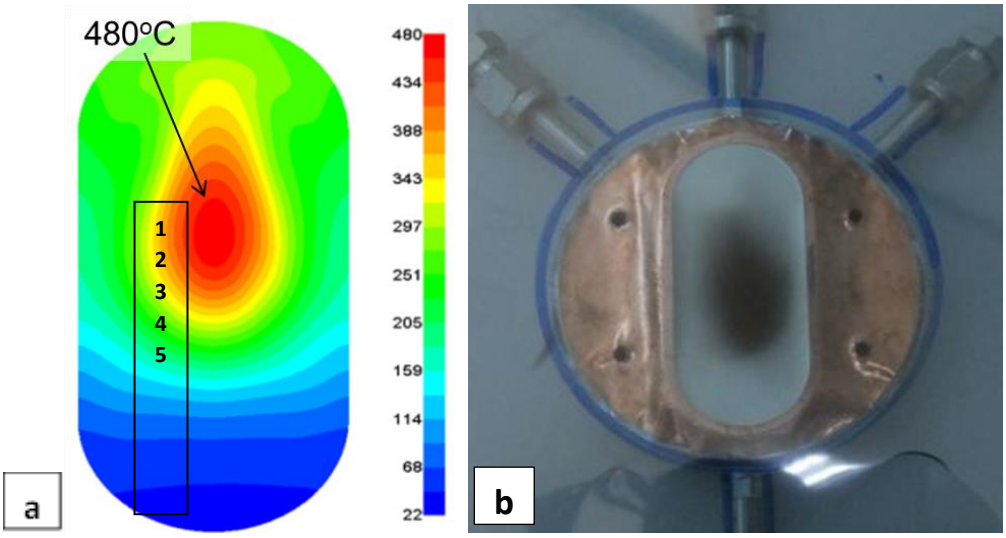

Figure 1. (a) Simulated foil temperature during irradiation and **(b)** auto-radiography of the irradiated foil on the target holder after irradiated.

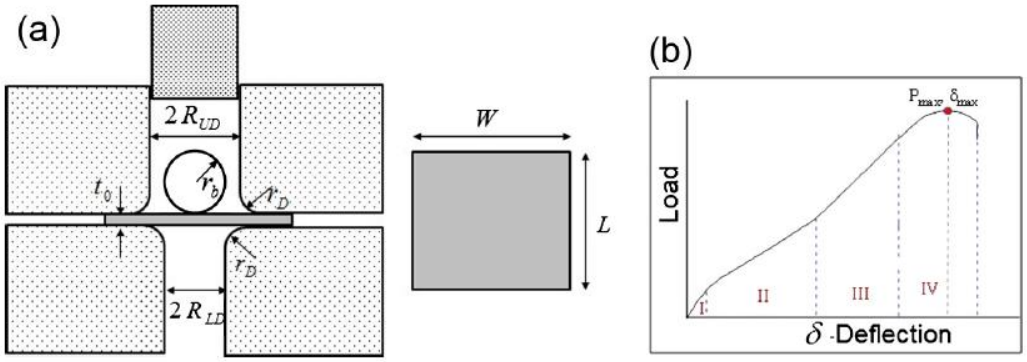

Figure 2. (a) Schematic apparatus for SPT, **(b)** typical curve of load vs. deflection; I—Elastic behavior, II—Plastic behavior (strain hardening), III—Plastic membrane stretching, and IV—plastic instability.

3. Results

The SPT load & displacement curves are shown in Figures 3, for the un-irradiated foil; the irradiated foil at 3.6 MeV, 310 μA of protons during 3 hours (case 1), and the irradiate foil at 3.6 MeV, 250 μA of protons during 40 hours (case 2). Figure 4 shows respectively energy to fracture for each case. The displacement per atom (DPA) per collision for the 3.6 MeV proton energy of approximately 8.5/Angstron is 0.044 for case 1 and 0.477 for case 2.

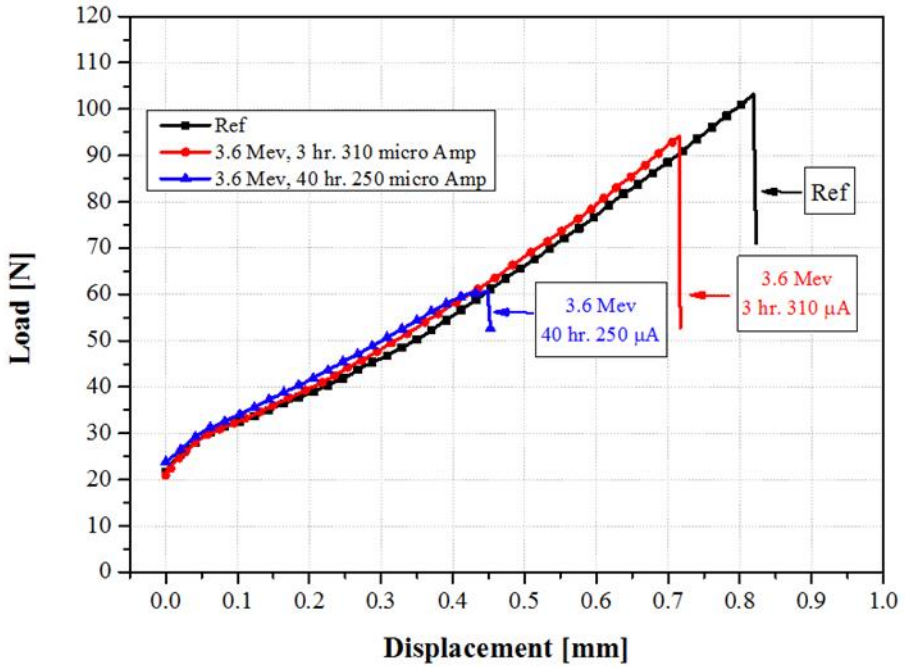

Figure 3. Comparison of the Small Punch Test results presenting load vs. displacement of as received foil and the irradiated foils in zone 1 as shown in figure 1a.

It can be seen in figure 2b that the curve obtained by SPT technique for each one of the foils condition, three regions were apparent: I—elastic, II—strain hardening, and III—membrane stretching up to failure which indicates plastic instability. When the failure occurs in the membranes the load dropped sharply. Cross section metallography using SEM reviled that more than 10 equiaxed grains presence across the thickness.

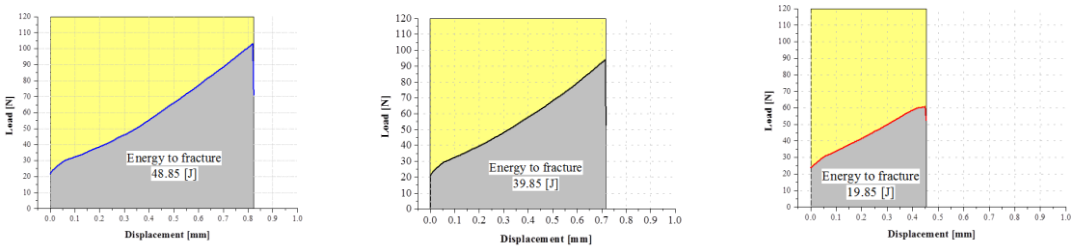

(a) (b) (c)

Figure 4. Energy to fracture: **(a)** for the as received foil - un-irradiated, 48 [J], **(b)** – 3.6 MeV, 310 μm proton during 3 hours, 39.85 [J], and **(c)** .6 MeV, 250 μm proton during 40 hours, 19.85 [J].

The maximal load for the SS316L un-irradiated foils with 25 μm thickness achieved the highest value of 100 N as shown in figure 3. Figure 5a-c exhibits the fracture failure area close to the stretching zone of the un-irradiated foil (5a) and for the low irradiated foil (5b - 3 hours). The characteristics of the rupture are consistent with the failure of a membrane as shown in previous works [14-15]. In contrast, the foil that was exposed to 40 hours of radiation (5c), the rupture was started on the center top of the cap (none shown).

The irradiated foils figure 5 (b) and (c) shown dislocation channels intersecting the surface of the austenitic stainless steel 316L attributed to the plastic strain and the irradiation. Furthermore, for the high irradiated sample in figure 5c, the fracture was developed in the channels by a zig-zag fracture mode (see red circle).

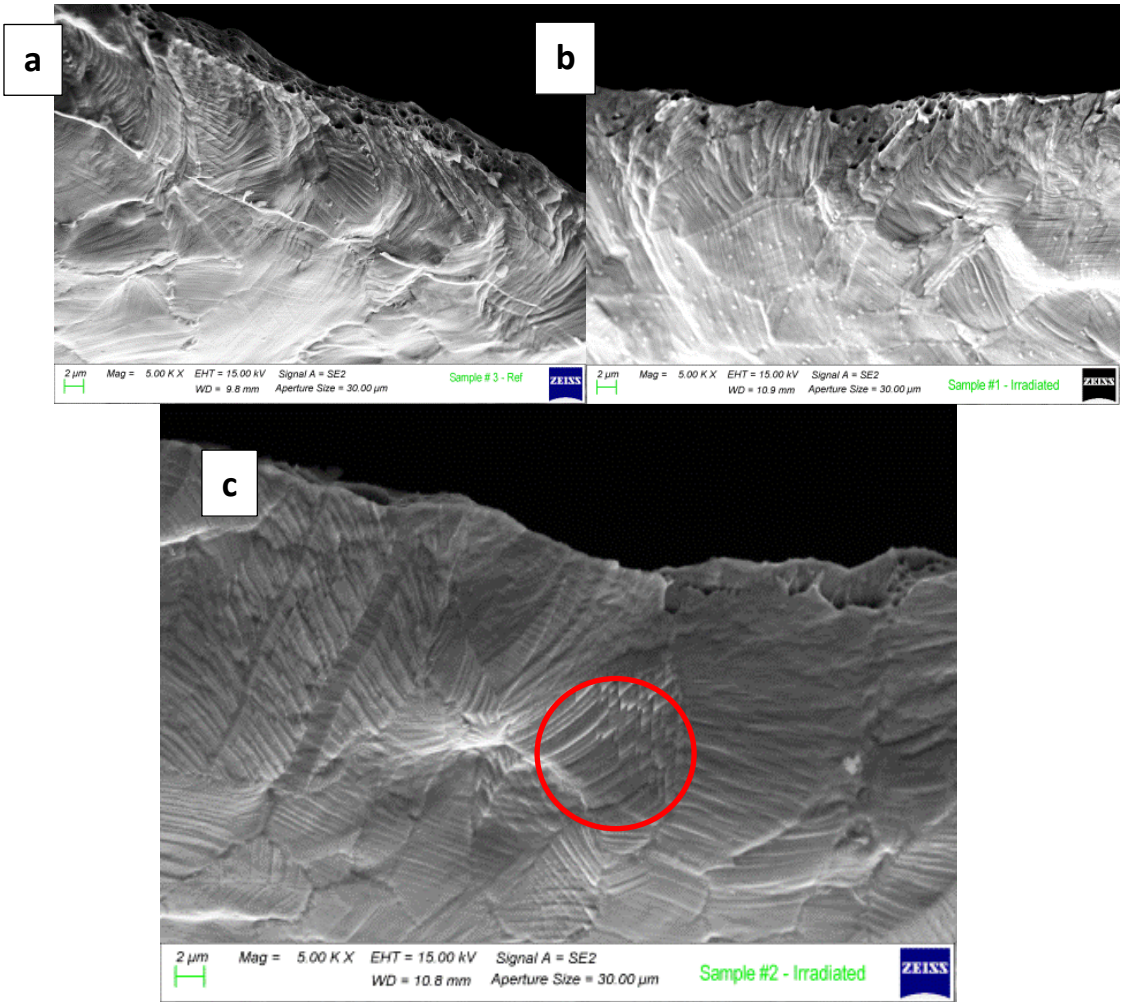

Figure 5. Zoom in on the stretched area close to the cross section fracture for the as received foil **(a)** - un-irradiated foil, **(b)** – 3.6 MeV, 310 μm proton during 3 hours, and **(c)** 3.6 MeV, 250 μm proton during 40 hours.

4. Discussion

Microstructure evolution during irradiation of a metal is controlled by the migration defect fractions of vacancies and interstitials. Irradiated metals exhibit a loss of ductility and a loss of work hardening. The loss of uniform ductility and the work hardening are due to the interaction between dislocations and the irradiated microstructure. Dislocation loops resulting from vacancy and interstitial condensation are created from clusters of defects and either shrink or grow depending on the flux of defects reaching the critical defect volume due to the radiation. Once the critical defect volume has been reached, the critical size under irradiation, the dislocation loops interacts with the network dislocation density. Deformation twinning or mechanical twinning is a localized deformation mechanism caused by partial dislocations. The low stacking fault energy in FCC metals and the deformation by twins contribute to the glide of Shockley partial dislocation on the same sign on successive {111} planes. By high shear strain, the defects due to the radiations are cleared by glide of the partial dislocations. Koyama et al. [16] report that the presences of hydrogen bring about quasi-cleavage fracture behavior in a single crystalline type of SS316L that has FCC structure. The deformation induced plate like products along the two specific planes in the <111> orientation with hydrogen charging. Some of the fracture edges are very similar to the fracture observed in figure 5c. They report [16], that the plate like products along the two specific planes are identified as the deformation twins along the two different {111} twinning plates. The study concluded that the obtained fracture surface depend on the crystallographic orientation and the degree of degradation on the tensile properties in the <111> tensile direction that is larger than the obtained in the <001> tensile orientation. They attribute this change to the higher flow stress and the formation of martensite at the intersections of the deformation twins. In this study the crack propagation path obtained is with a zigzag shape as observed in figure 5c. This effect is due to multiple deformation twinning and smooth when only a small amount of deformation twins appear on a single {111} twinning plane. We assume that in irradiated samples there are similar behavior as shown in figure 5b (zigzags in the pre-crack stage) and in figure 5c (zigzags after the crack was created), attributed by the accumulation of interstitials, vacancies and remained protons or hydrogen due to the irradiation damage that effects on the partial dislocation glide and reduces the ductility of the metal. The electron microscopy observations (SEM) revealed high cross slips and pseudo-cleavage density after irradiation to high energy.

Future research on TEM characterization should be done to define the deformation mechanism on two axes as evolved in the SPT technique and to characterize the proper mechanism that leads to loss of ductility and a loss of work hardening in the irradiated materials.

5. Conclusions

The changes in microstructure due to the expose of the SS316L under proton irradiation can explain the major changes in the mechanical properties obtained by the SPT technique.

The irradiated samples show consistent degradation on the mechanical behavior in comparison to the non-irradiated sample. Maximum load, ductility and work hardening range decrease by irradiation. The highest degradation was observed in the foil exposed to 3.6 MeV, 250 μm of proton during 40 hours.

The fractography shown dislocations and twins attributed by the accumulation of interstitials, vacancies and remained protons due to the irradiation damage that effects on the partial dislocation glide and reduces the ductility of the metal.

Acknowledgments: This work was part of the research plan of the Soreq Applied Research Accelerator Facility (SARAF). The authors thank the SARAF team named in reference 1.

References

1. Mardor, I.; Aviv, O.; Avrigeanu, M.; Berkovits, D.; Dahan, A.; Dickel, T.; Eliyahu, I.; Gai, M.; Gavish-Segev, I.; Halfon, S.; Hass, M.; Hirsh, T.; Kaiser, B.; Kijel, D.; Kreisel, A.; Mishnayot, Y.; Mukul, I.; Ohayon, B.; Paul, M.; Perry, A.; Rahangdale, H.; Rodnizki, J.; Ron, G.; Sasson-Zukran, R.; Shor, A.; Silverman, I.; Tessler, M.; Vaintraub, S.; and Weissman, L.; "The Soreq Applied Research Accelerator Facility (SARAF) – Overview, Research Programs and Future Plans", [*physics.ins-det*] (submitted as an invited review to *European Physics Journal A*, on 19 Jan 2018 (*v1*), last revised 23 Jan 2018) Available online: arXiv:1801.06493 (accessed on 23 Jan 2018).

2. Guduru, R.K.; Darling, K.A.; Kishore, R.; Scattergood, R.O.; Koch, C.C.; Murty, K.L. Evaluation of mechanical properties using shear–punch testing. *Mater. Sci. Eng. A*, **2005**, *vol. 395*, 307–314.
3. Guduru, R.K.; Wong, P.Z.; Darling, K.A.; Koch, C.C.; Murty, K.L.; Scattergood, R.O. Determination of activation volume in nanocrystalline Cu using the shear punch test. *Adv. Eng. Mater.* **2007**, *vol. 9*, 855–859.
4. Hamilton, M.; Toloczko, M. Effect of low temperature irradiation on the mechanical properties of ternary V–Cr–Ti alloys as determined by tensile tests and shear punch tests. *J. Nucl. Mater*. **2000**, *vol. 283*, 488–491.
5. Toloczko, M.B.; Kurtz, R.J.; Hasegawa, A.; Abe, K. Shear punch tests performed using a new low compliance test fixture. *J. Nucl. Mater*. **2002**, *vol. 307*, 1619–1623.
6. Hankin, G.L.; Toloczko, M.B.; Hamilton, M.L.; Garner, F.A.; Faulkner, R.G., Shear punch testing of 59 Ni isotopically-doped model austenitic alloys after irradiation in FFTF at different He/dpa ratios. *J. Nucl. Mater.* **1998,** *vol. 258*, 1657–1663.
7. Goyal, S.; Karthik, V.; Kasiviswanathan, K.V.; Valsan, M.; Rao, K.B.; Raj, B. Finite element analysis of shear punch testing and experimental validation. *Mater. Des.* **2010,** *vol. 31*, 2546–2552
8. ASTM- American Society for Testing and Materials. Ball Punch Deformation of Metallic Sheet Material; ASTM-E643; American Society for Testing and Materials: West Conshohocken, PA, USA, 1987; pp. 885–888.
9. García, T.E.; Rodríguez, C.; Belzunce, F.J.; Suárez, C. Estimation of the mechanical properties of metallic materials by means of the small punch test. *J. Alloys Compd*. **2014**, *vol. 582*, 708–717.
10. Baik, J.-M.; Kameda, J.; Buck, O., Development of small punch tests for ductile-brittle transition temperature measurement of temper embrittled Ni-Cr steels. *The Use of Small-Scale Specimens for Testing Irradiated Material*; Corwin, W.R., Lucas, G.E., Eds.; ASTM-STP 888; American Society for Testing and Materials: West Conshohocken, PA, USA, 1983; pp. 92–111.
11. Mao, X.; Takahashi, H. Development of a further-miniaturized specimen of 3 mm diameter for TEM disk (ø 3 mm) small punch tests. *J. Nucl. Mater*. **1987**, *vol. 150*, 42–52.
12. Klein, M.; Hadrboletz, A.; Weiss, B.; Khatibi, G. The 'size effect' on the stress–strain, fatigue and fracture properties of thin metallic foils. *Mater. Sci. Eng. A*, **2001**, *vol. 319*, 924–928.
13. Matocha, K.; Hurst, R. The European Code of Practice for Small Punch testing—where do we go from here. In Proceedings of the 1st International Conference on Determination of Mechanical Properties of Materials by Small Punch and other Miniature Testing Techniques, Ostrava, Czech Republic, 30 August–2 September 2010.
14. Haroush, S., Priel, E., Moreno, D., Busiba, A., Silverman, I., Turgeman, A., Shneck, R., and Gelbstein, Y., Evaluation of the mechanical properties of SS-316L thin foils by small punch testing and finite element analysis. *Mater. Des*. **2015**, *vol. 83*, 75–84.
15. Haroush, S., Moreno, D., Silverman, I., Turgeman, A., Shneck, R. and Gelbstein, Y., The Mechanical Behavior of HAVAR Foils Using the Small Punch Technique, *Materials* **2017**, *vol. 10*, 491; DOI:10.3390/ma10050491.
16. Koyama, M., Akiyama, E., Sawaguchi, T., Ogawa, K., Kireeva, I. V., Chumlyakov, Y.I. and Tsuzaki, K., Hydrogen Assisted Quasi-Cleavage Fracture in Single Crystalline Type 316 Austenitic Stainless Steel, *Corrosion Science* **2013** *vol. 75*, 345-353.